Organometallics **1999,** *18,* 4107−4113

Titanium and Zirconium Complexes with the New Ancillary Diamido Ligand *N,N′*-Bis(trimethylsilyl)amidobenzylamido(2−): Syntheses, Structures, and α-Olefin Polymerization Activities

You-Moon Jeon, Jungseok Heo, Won Mok Lee, Taihyun Chang, and Kimoon Kim*

Department of Chemistry and National Creative Research Initiative Center for Smart Supramolecules, Pohang University of Science and Technology, San 31 Hyojadong, Pohang 790-784, South Korea

Received February 22, 1999

Using the disymmetric *N,N′*-bis(trimethylsilyl)aminobenzylamine (H_2MABA; **1**) ligand, the new group 4 metal complexes (MABA)$TiCl_2$ (**2**), (MABA)$TiMe_2$ (**3**), (MABA)$Ti(CH_2Ph)_2$ (**4**), (MABA)$ZrCl_2$ (**5**), and $(MABA)_2Zr$ (**6**) were prepared. X-ray crystal structures of **2**, **4**, and **6** were determined. The crystal structure of **2** suggests that an agostic interaction between the titanium metal center and benzylic protons exists in the solid state. However, the agostic interaction is not sustained in solution, as indicated by NMR spectroscopy. Complexes **2** and **5**, activated by MMAO, and **4**, activated by $B(C_6F_5)_3$, have moderate catalytic activities for the polymerization of α-olefins.

Introduction

Group 4 metal complexes containing chelating diamido or dialkoxo ligands have attracted much attention[1−10] as potential catalysts for the polymerization of terminal olefins because of their close relationship with the well-known metallocene and cyclopentadienyl−amide complexes.[11] Not only are such noncyclopentadienyl ligands easily accessible but also their metal complexes often exhibit novel types of polymerization activities such as living polymerization of α-olefins. For example, titanium complexes with propylene-bridged aryl-substituted diamido ligands reported by McConville catalyze the living polymerization of terminal olefins at room temperature.[1] Zirconium complexes of oxo-bridged dianiline derivatives reported by Schrock are also good catalyst precursors for the living polymerization of terminal olefins.[3c] We also recently reported zirconium complexes containing the novel diamido ancillary ligand 2,2′-ethylenebis(*N,N′*-(triisopropylsilyl)aniline) (EBT^{i}P), which exhibit remarkable activities of living polymerization of terminal olefins.[10] Here we report titanium and zirconium complexes of another new ancillary ligand, *N,N′*-bis(trimethylsilyl)amidobenzylamido $(MABA)^{2-}$, and their catalytic activities of olefin polymerization.

Results and Discussion

Titanium Complexes. The free base ligand H_2(MABA) (**1**) was synthesized in a moderate yield by the reaction of lithiated 2-aminobenzylamine and 2 equiv of trimethylsilyl chloride in THF. Reaction of the lithium salt of **1** with $TiCl_4(THF)_2$ in refluxing toluene produces

---

[1] (a) Scollard, J. D.; McConville, D. H.; Vittal, J. J. *Organometallics* **1997**, *16*, 1810. (b) Scollard, J. D.; McConville, D. H. *J. Am. Chem. Soc.* **1996**, *118*, 10008. (c) Scollard, J. D.; McConville, D. H.; Payne, N. C.; Vittal, J. J. *Macromolecules* **1996**, *29*, 5241. (d) Guerin, F.; McConville, D. H.; Vittal, J. J. *Organometallics* **1995**, *14*, 3154.

[2] (a) Britovsek, G. J. P.; Gibson, V. C.; Duncan, F. W. *Angew. Chem., Int. Ed.* **1999**, *38*, 428. (b) Tsuie, B.; Swenson, D. C.; Jordan, R. F. *Organometallics* **1997**, *16*, 1392. (c) Lee, C. H.; Na, Y.-H.; Park, S. J.; Park, J. W. *Organometallics* **1998**, *17*, 3648.

[3] (a) Schrock, R. R.; Schattenmann, F.; Aizenberg, M.; Davis, M. D. *Chem. Commun.* **1998**, 199. (b) Warren, T. H.; Schrock, R. R.; Davis, W. M. *Organometallics* **1996**, *15*, 562. (c) Baumann, R.; Davis, W. M.; Schrock, R. R. *J. Am. Chem. Soc.* **1997**, *119*, 3830. (d) Schrock, R. R.; Seidel, S. W.; Schrodi, Y.; Davis, W. M. *Organometallics* **1999**, *18*, 428. (e) Graf, D. D.; Schrock, R. R.; Davis, W. M.; Stumpf, R. *Organometallics* **1999**, *18*, 428.

[4] (a) Clark, H. C. S.; Cloke, F. G. N.; Hitchcock, P. B.; Love, J. B.; Wainwright, A. P. *J. Organomet. Chem.* **1995**, *501*, 333. (b) Cloke, F. G. N.; Hitchcock, P. B.; Love, J. B. *J. Chem. Soc., Dalton Trans.* **1995**, 25. (c) Cloke, F. G.; Geldbach, T. J.; Hichcoke, P. B.; Love, J. B. *J. Organomet. Chem.* **1995**, *506*, 343.

[5] (a) Horton, A. D.; de With, J. *Organometallics* **1997**, *16*, 5424. (b) Horton, A. D.; de With, J.; van der Linden, A. J.; van de Weg, H. *Organometallics* **1996**, *15*, 2672. (c) Horton, A. D.; de With, J. *Chem. Commun.* **1996**, 1375. 6.

[6] Tinkler, S.; Deeth, R. J.; Duncalf, D. J.; McCamley, A. *Chem. Commun.* **1996**, 2623.

[7] Aoyagi, K.; Gantzel, P. K.; Kalai, K.; Tilley, T. D. *Organometallics* **1996**, *15*, 923.

[8] Pritchett, S.; Gantzel, P.; Walsh, P. J. *Organometallics* **1997**, *16*, 5130.

[9] Male, N. A. H.; Thornton-Pett, M.; Bochmann, M. *J. Chem. Soc., Dalton Trans.* **1997**, 2487.

[10] Jeon, Y.-M.; Park, S. J.; Heo, J.; Kim, K. *Organometallics* **1998**, *17*, 3161.

[11] (a) Guram, A. S.; Jordan, R. F. In *Comprehensive Organometallic Chemistry*, 2nd ed.; Lappert, M. F., Ed.; Pergamon: Oxford, U.K., 1995; Vol. 4, pp 589−625. (b) McKnight, A. L.; Waymouth, R. M. *Chem. Rev.* **1998**, *98*, 2587. (c) Kaminsky, W. *J. Chem. Soc., Dalton Trans.* **1998**, 1413. (d) Brintzinger, H. H.; Fischer, D.; Mulhaupt, R.; Rieger, B.; Waymouth, R. M. *Angew. Chem., Int. Ed. Engl.* **1995**, *34*, 1143. (e) Mohring, P. C.; Coville, N. J. *J. Organomet. Chem.* **1994**, *479*, 1.

10.1021/om990121b CCC: $15.00

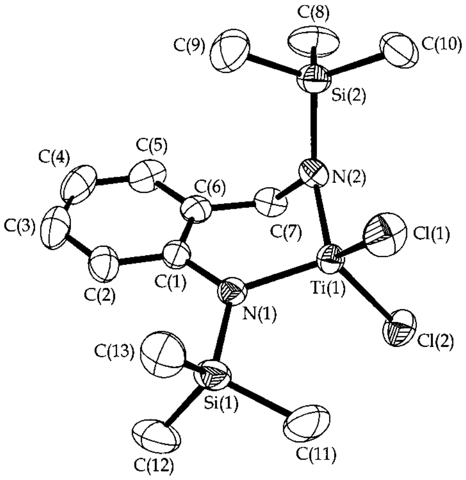

Figure 1. X-ray crystal structure of **2**. Only one of the two independent molecules (molecule 1) is depicted.

Table 1. Selected Bond Distances (Å) and Bond Angles (deg) for 2

molecule 1		molecule 2	
Ti(1)−N(1)	1.895(2)	Ti(2)−N(3)	1.904(2)
Ti(1)−N(2)	1.825(2)	Ti(2)−N(4)	1.827(2)
Ti(1)−Cl(1)	2.2316(11)	Ti(2)−Cl(3)	2.2272(11)
Ti(1)−Cl(2)	2.2714(12)	Ti(2)−Cl(4)	2.2697(13)
Ti(1)···C(7)	2.506(3)	Ti(2)···C(20)	2.500(3)
Ti(1)···H(7A)	2.36(3)	Ti(2)···H(20A)	2.33(3)
N(1)−Ti(1)−N(2)	99.25(9)	N(3)−Ti(2)−N(4)	99.25(9)
Cl(1)−Ti(1)−Cl(2)	112.17(4)	Cl(3)−Ti(2)−Cl(4)	112.91(4)
Ti(1)−N(2)−C(7)	97.36(15)	Ti(2)−N(4)−C(20)	97.16(15)
Ti(1)−N(2)−Si(2)	140.34(12)	Ti(2)−N(4)−Si(4)	139.79(13)
Si(2)−N(2)−C(7)	119.39(16)	Si(4)−N(4)−C(20)	120.11(17)

the dark red product (MABA)$TiCl_2$ (**2**) (eq 1). The

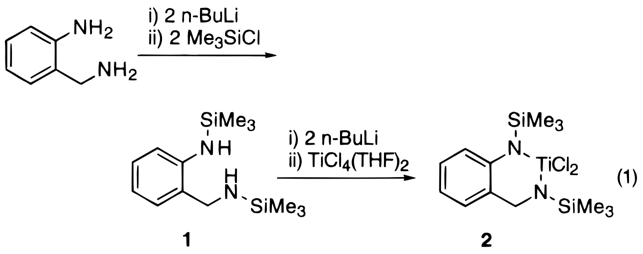

(1)

product has been characterized by $^1H/^{13}C$ NMR spectroscopy, mass spectrometry, elemental analysis, and X-ray crystallography. Although the reaction proceeds almost quantitatively, as indicated by ^1H NMR spectroscopy, the isolation yield is much lower because of the high solubility of the product in most hydrocarbon solvents, including pentane.

Single crystals of **2** suitable for X-ray crystallography were obtained from a chilled pentane solution. The asymmetric unit contains two independent molecules with almost identical structures, one of which is shown in Figure 1. Selected bond distances and angles are summarized in Table 1. No unusual bond parameters are observed. The titanium ion is coordinated by two nitrogen atoms and two chloride ions in a distorted-tetrahedral geometry. The N−Ti−N angle (99.25(9)° for both molecule 1 and molecule 2) is quite similar to that in McConville's catalyst ([$ArNCH_2CH_2CH_2NAr$]$TiCl_2$ (Ar = 2,6-$^iPr_2C_6H_3$; 99.2(2)°)[1c] but much larger than that in *o*-$C_6H_4(NSi^iPr_3)_2TiCl_2$ (92.6(2)°).[7] This difference may be due to the fact that **2** and McConville's compound have a six-membered metallacycle while *o*-$C_6H_4(NSi^iPr_3)_2TiCl_2$ contains a five-membered chelate ring. The Cl−Ti−Cl angle (112.17(4)° for molecule 1 and 112.91(4)° for molecule 2) is larger than that in McConville's complex (107.77(9)°), presumably due to the smaller substituent on the nitrogen atom in **2**. A planar geometry of the nitrogen atoms indicates that the sp^2-hybridized atoms have $p\pi-d\pi$ interactions with the metal center.

Interestingly, the bond angles Ti(1)−N(2)−C(7) (molecule 1) and Ti(2)−N(4)−C(20) (molecule 2) in the six-membered titanacycles are small (97.36(15)° and 97.16(15), respectively) and the interatomic distances Ti(1)···C(7) (molecule 1) and Ti(2)···C(20) (molecule 2) are short (2.506(3) and 2.500(3) Å, respectively), which suggests that there is an agostic (three-center−two-electron) interaction between C(7)−H and Ti(1) (molecule 1) and C(20)−H and Ti(2) (molecule 2).[12,13] In the ^1H NMR spectrum of **2** at ambient temperature, the benzylic protons resonate at 5.32 ppm as a singlet in chloroform-*d*, which is considerably shifted to lower field compared to those of the free ligand **1** and the Ti complex **4**, 3.86 (singlet) and 4.58 (singlet) ppm, respectively (vide infra). However, the large C−H coupling constant for C(7)−H (or C(20)−H) (137.6 Hz) in **2** suggests that the agostic interaction between the Ti and C(7)−H (or C(20)−H) is not sustained in solution. Furthermore, the signal for the benzylic protons remains as a singlet even at −90 °C in dichloromethane-d_2 or toluene-d_8 solution, indicating a rapid fluxional behavior even at the low temperature.

The complex **2** was treated with MeMgI in ether solution to give the dimethyl derivative **3** (eq 2).

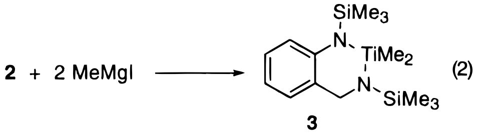

(2)

Although the reaction produces the desired product almost quantitatively, as indicated by NMR spectroscopy, we failed to isolate analytically pure crystalline product. The product was isolated as a sticky solid which was difficult to recrystallize due to its high solubility even in pentane.

The dibenzyltitanium complex **4** was synthesized analogously by the reaction of **2** and benzylmagnesium chloride in ether solution at room temperature (eq 3).

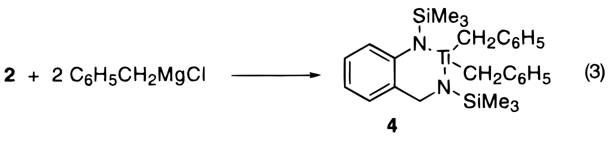

(3)

In the ^1H NMR spectrum, the benzylic protons of the

---

[12] (a) Scherer, W.; Priermeier, T.; Haaland, A.; Volden, V.; McGrady, G. S.; Downs, A. J.; Boese, R.; Blaser, D. *Organometallics* **1998**, *17*, 4406. (b) Scherer, W.; Hieringer, W.; Spiegler, M.; Sirsch, P.; McGrady, G. S.; Downs, A. J.; Haaland, A.; Pedersen, B. *Chem. Commun.* **1998**, 2471. (c) Braga, D.; Grepioni, F.; Biradha, K.; Desiraju, G. R. *J. Chem. Soc., Dalton Trans.* **1996**, 3925. (d) Crabtree, R. H. *Angew, Chem., Int. Ed. Engl.* **1993**, *32*, 789. (e) Brookhart, M.; Green, M. *J. Organomet. Chem.* **1983**, *250*, 395. (f) Ujaque, G.; Cooper, A. C.; Maseras, F.; Einstein, O.; Caulton, K. G. *J. Am. Chem. Soc.* **1998**, *120*, 361.

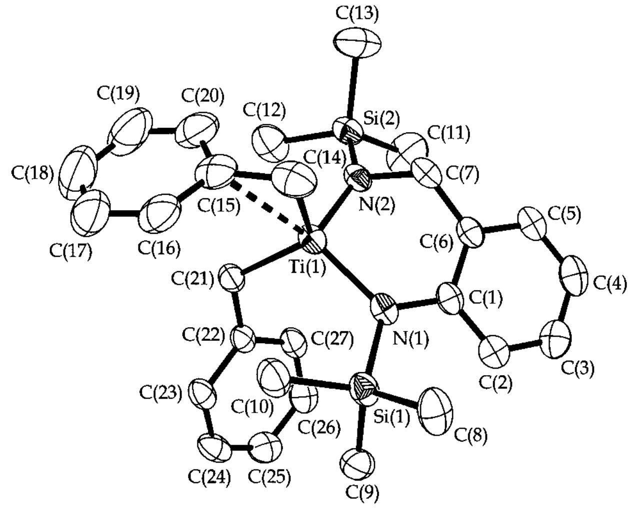

Figure 2. X-ray crystal structure of **4**. Only one of the two independent molecules (molecule 1) is depicted.

Table 2. Selected Bond Distances (Å) and Bond Angles (deg) for 4

molecule 1		molecule 2	
Ti(1)−N(1)	1.942(3)	Ti(2)−N(3)	1.934(3)
Ti(1)−N(2)	1.873(3)	Ti(2)−N(4)	1.854(3)
Ti(1)−C(14)	2.138(4)	Ti(2)−C(44)	2.111(4)
Ti(1)−C(21)	2.114(4)	Ti(2)−C(51)	2.129(4)
Ti(1)···C(7)	2.614(4)	Ti(2)···C(37)	2.597(4)
Ti(1)···C(15)	2.647(4)	Ti(2)···C(45)	3.188(4)
Ti(1)···C(22)	3.110(4)	Ti(2)···C(52)	2.992(4)
N(1)−Ti(1)−N(2)	99.84(13)	N(3)−Ti(2)−N(4)	99.61(13)
C(14)−Ti(1)−C(21)	120.7(2)	C(44)−Ti(2)−C(51)	109.2(2)
Ti(1)−N(1)−C(1)	121.8(2)	Ti(2)−N(3)−C(31)	120.3(2)
Ti(1)−N(2)−C(7)	101.0(2)	Ti(2)−N(4)−C(37)	100.9(2)
Ti(1)−C(14)−C(15)	92.5(3)	Ti(2)−C(44)−C(45)	123.6(3)
Ti(1)−C(21)−C(22)	118.5(2)	Ti(2)−C(51)−C(52)	110.6(3)

chelate ring appear at 4.58 ppm as a singlet signal while the metal-bound benzylic protons appear at 2.43 and 2.59 ppm as two doublets. No decoalescence of the chelate benzylic proton signal was observed, even at −60 °C in chloroform-*d* solution. Although complex **4** is a gelatinous solid at room temperature, slow cooling of a pentane solution of **4** to −50 °C produced single crystals suitable for X-ray work. The unit cell contains two independent molecules with similar geometrical parameters. The molecular structure of one of them (molecule 1) is depicted in Figure 2, and selected bond distances and bond angles are summarized in Table 2. The average Ti−N distances are 1.908(3) Å (molecule 1) and 1.884(3) Å (molecule 2). The N−Ti−N angles are 99.84(13)° (molecule 1) and 99.61(13)° (molecule 2). The Ti(1)−C(14) and Ti(1)−C(21) distances are 2.138(4) and 2.114(4) Å, respectively, and the C(14)−Ti(1)−C(21) angle is 120.7(2)° for molecule 1. Similar metric parameters are found for molecule 2. In contrast to **2**, no agostic interaction between the benzylic hydrogen atoms of the chelate ring and the metal center is evident in this structure: Ti(1)···C(7) = 2.614(4) Å, Ti(1)−N(2)−C(7) = 101.0(2)° (molecule 1) and Ti(2)···C(37) = 2.597(4) Å, Ti(2)−N(4)−C(37) = 100.9(2)° (molecule 2). It is also interesting to note that, in molecule 1, one of the benzyl groups attached to the metal center has a normal Ti−CH_2−Ph angle (Ti(1)−C(21)−C(22) = 118.5(2)°), whereas the other benzyl group has an acute Ti−CH_2−Ph angle (Ti(1)−C(14)−C(15) = 92.5(3)°) and a short Ti···C_{ipso} distance (Ti(1)···C(15) = 2.647(4) Å). This structure suggests that the former benzyl group is bound to the metal center in an η^1 fashion whereas the latter is bound in an η^2 fashion. A similar η^2 coordination mode of the benzyl groups has been observed in other Ti complexes: $Ti(CH_2Ph)_4$ (Ti−C−C_{ipso} = 88(2), 98(2)°, Ti···Ph_{ipso} = 2.61(2), 2.81(3) Å);[14a,b] $[\{Ti(CH_2Ph)_3\}_2(\mu\text{-}\eta^5{:}\eta^5\text{-}C_{10}H_8)]$ (Ti−C−C_{ipso} = 90.9(3)°, Ti···Ph_{ipso} = 2.611(4) Å);[14c] μ-[*o*-$(CH_2)_2C_6H_4$]{Cp*Ti[*o*-$(CH_2)_2C_6H_4$]}$_2$ (Ti−C−C_{ipso} = 84.7(8)°, Ti···Ph_{ipso} = 2.47(1) Å);[14d] (Ben)Ti(CH_2Ph)Cl (Ti−C−C_{ipso} = 87.0(5)°, Ti···Ph_{ipso} = 2.500(8) Å).[14e] However, only an η^1 coordination mode of the benzyl groups is observed in molecule 2: Ti(2)···C(45) = 3.188(4) Å, Ti(2)···C(52) = 2.992(4) Å. Furthermore, the η^2-benzyl interaction is not observed in solution. As mentioned above, the metal-bound benzylic protons in **4** show a diastereotopic AB pattern with δ_A 2.43, δ_B 2.59, and J_{A-B} = 10.5 Hz. This large geminal coupling constant suggests that the benzyl ligand has an sp^3-hybridized methylene carbon. In the ^{13}C NMR spectrum, the Ti−CH_2 resonance occurs farther downfield (82.5 ppm, J_{C-H} = 123.4 Hz) compared to those of previously known (η^2-benzyl)titanium complexes (δ <75 ppm, J_{C-H} > 130 Hz).[15] These NMR data suggest that such an η^2-benzyl interaction is not sustained in solution.

Zirconium Complexes. At the outset of this work we expected to synthesize the dichlorozirconium complex (MABA)$ZrCl_2$ (**5**) in a way analogous to that for the corresponding titanium complex (MABA)$TiCl_2$ (**2**). However, the reaction of the dilithium salt of **1** and $ZrCl_4(THF)_2$ in refluxing toluene results in $(MABA)_2Zr$ (**6**) (eq 4), instead.

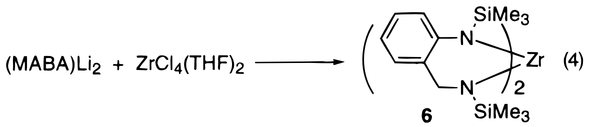

The first evidence for the formation of the 2:1 complex **6** came from its ^1H NMR spectrum. In contrast to the 1:1 complexes **2**−**4**, the benzylic protons in **6** show a typical AB spin pattern at 4.23 and 4.54 ppm (doublet, J_{H-H} = 15.3 Hz) in chloroform-*d* solution at room temperature. For unequivocal structural characterization we decided to determine the structure by X-ray crystallography. Single crystals of **6** suitable for X-ray work were obtained from a chilled pentane solution. The asymmetric unit contains two independent molecules

---

(13) Although accurate positions of hydrogen atoms are difficult to obtain by X-ray diffraction methods, the hydrogen atoms attached to C(7) and C(20) were located from the difference electron density map and refined isotropically. The short Ti···H distances (Ti(1)···H(7A) = 2.36(3) Å (molecule 1), Ti(2)···H(20A) = 2.33(3) Å (molecule 2)) also support the agostic interaction in the solid state.

(14) For leading references for titanium−benzyl bonding, see: Bochmann, M. In *Comprehensive Organometallic Chemistry*, 2nd ed.; Lappert, M. F., Ed.; Pergamon: Oxford, U.K., 1995; Vol. 4, pp 273−431. See also: (a) Bassi, I. W.; Allegra, R.; Scordamaglia, G.; Chioccola, G. *J. Am. Chem. Soc.* **1971**, *93*, 3787. (b) Davies, G. R.; Jarvis, J. A. J.; Kilbourn, B. T. *J. Chem. Soc. D.* **1971**, 1511. (c) Alvaro, L. M.; Flores, J. C.; Royo, P.; Pellinghelli, M. A.; Tiripicchio, A. *Organometallics* **1992**, *11*, 3301. (d) Mena, M.; Royo, P.; Serrano, R.; Pellinghelli, M. A.; Tiripicchio, A. *Organometallics* **1989**, *8*, 476. (e) Warren, T. H.; Schrock, R. R.; Davis, W. M. *Organometallics* **1996**, *15*, 562.

(15) (a) Latesky, S. L.; McMullen, A. K.; Niccolai, G. P.; Rothwell, I. P.; Huffman, J. C. *Organometallics* **1985**, *4*, 902. (b) Hughes, A. K.; Meetsma, A.; Teuben, J. H. *Organometallics* **1993**, *12*, 1936.

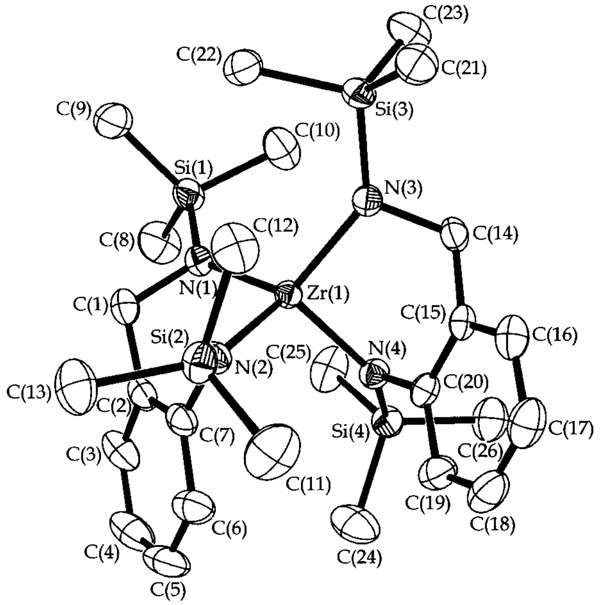

Figure 3. X-ray crystal structure of **6.** Only one of the two independent molecules (molecule 1) is depicted.

Table 3. Selected Bond Distances (Å) and Bond Angles (deg) for 6

molecule 1		molecule 2	
Zr(1)−N(1)	2.0543(16)	Zr(2)−N(5)	2.0532(16)
Zr(1)−N(2)	2.0949(16)	Zr(2)−N(6)	2.0950(16)
Zr(1)−N(3)	2.0554(16)	Zr(2)−N(7)	2.0536(15)
Zr(1)−N(4)	2.0884(16)	Zr(2)−N(8)	2.0926(16)
Zr(1)···C(7)	2.715(2)	Zr(2)···C(33)	2.7344(19)
Zr(1)···C(20)	2.7306(19)	Zr(2)···C(46)	2.7217(19)
N(1)−Zr(1)−N(2)	98.52(6)	N(5)−Zr(2)−N(6)	98.31(6)
N(1)−Zr(1)−N(3)	115.08(6)	N(5)−Zr(2)−N(7)	113.84(6)
N(1)−Zr(1)−N(4)	118.22(6)	N(5)−Zr(2)−N(8)	119.03(6)
N(2)−Zr(1)−N(3)	119.59(6)	N(6)−Zr(2)−N(7)	119.53(6)
N(2)−Zr(1)−N(4)	108.58(6)	N(6)−Zr(2)−N(8)	109.03(6)
N(3)−Zr(1)−N(4)	97.92(6)	N(7)−Zr(2)−N(8)	98.32(6)
Zr(1)−N(1)−C(1)	107.67(12)	Zr(2)−N(5)−C(40)	108.51(11)
Zr(1)−N(2)−C(7)	99.05(12)	Zr(2)−N(6)−C(46)	99.29(11)
Zr(1)−N(3)−C(14)	108.04(12)	Zr(2)−N(7)−C(27)	108.11(11)
Zr(1)−N(4)−C(20)	100.09(11)	Zr(2)−N(8)−C(33)	100.04(11)

of **6** with nearly identical structures. The molecular structure of one of them (molecule 1) is shown in Figure 3, and selected bond distances and angles are listed in Table 3. No unusual bond parameters are observed. As we suspected, the Zr ion is coordinated by four nitrogen atoms of the two MABA ligands in a distorted-tetrahedral geometry. The Zr−N bond distances range from 2.054 to 2.095 Å. The aromatic amide has a longer Zr−N distance than the benzylic amide: e.g., Zr(1)−N(1) = 2.0543(16) Å; Zr(1)−N(2) = 2.0949(16) Å. The average bite angle of the ligand is 98.22(2)°. All the nitrogen atoms coordinated to zirconium have a trigonal-planar geometry. It is interesting to note that the bond angles Zr(1)−N(2)−C(7) (99.05(12)°) and Zr(1)−N(4)−C(20) (100.09(11)°) are considerably smaller than the angles Zr(1)−N(1)−C(1) (107.67(12)°) and Zr(1)−N(3)−C(14) (108.04(12)°).

The desired dichlorozirconium complex (MABA)$ZrCl_2$ (**5**) was finally prepared by the ligand redistribution reaction of **6** with 1 equiv of $ZrCl_4(THF)_2$ in refluxing toluene. The reaction was monitored by NMR spectroscopy. The two doublet signals of the benzylic protons of the chelate ring in **6** merged into a singlet peak in 3 days, which indicates formation of the dichlorozirconium complex **5** (eq 5). Complex **5** is a slightly yellow solid,

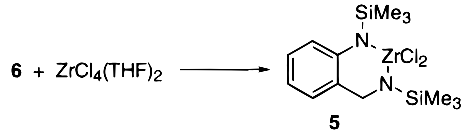

5

(5)

sparingly soluble in nonpolar hydrocarbon solvents but soluble in polar solvents such as diethyl ether, THF, dichloromethane, and toluene. In **5**, one THF molecule is coordinated to the zirconium metal center, as indicated by $^1H/^{13}C$ NMR spectroscopy and elemental analysis. A similar ligand redistribution reaction of [Ti-$(Me_3SiNCH_2CH_2NSiMe_3)_2$] with 1 equiv of $TiCl_4(THF)_2$ has been reported to produce the dichloro complex [Ti-$(Me_3SiNCH_2CH_2NSiMe_3)Cl_2$].[6]

This ligand redistribution reaction led us to examine the mechanism of formation of **2** by monitoring the reaction of the lithium salt of **1** with $TiCl_4(THF)_2$ (eq 1) by ^1H NMR spectroscopy. Interestingly, the NMR spectrum of the reaction mixture after 1 h reflux shows a doublet of doublets pattern for the benzylic protons of the chelate ring, as observed in **6**. However, only a singlet signal was observed after 3 h reflux. This observation suggests that, in this reaction, the 2:1 complex $(MABA)_2Ti$ forms first, which quickly undergoes a ligand redistribution reaction with remaining $TiCl_4(THF)_2$ to form the 1:1 complex **2** (eq 6). The 2:1 complex $(MABA)_2Ti$ appears to be less stable than the corresponding Zr complex **6**. The higher stability of the Zr complex appears to be due to the larger radius of the Zr ion. With these results we now can synthesize any of the 1:1 and 2:1 complexes of titanium and zirconium by controlling the reaction time and conditions carefully.

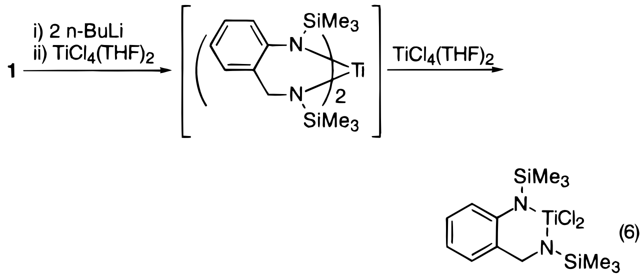

(6)

2

Polymerization. Complexes **2** and **5** activated by modified methylaluminoxane (MMAO) and **4** activated by $B(C_6F_5)_3$ have moderate catalytic activities for the polymerization of olefins. A summary of the polymerization results is shown in Table 4. Although their catalytic activities are not as high as those of the best known noncyclopentadienyl group 4 metal complexes such as McConville's Ti complexes,[1] Schrock's Zr complexes,[2c] and our $(EBT^iP)ZrMe_2$,[10] these systems are active catalysts for the polymerization of terminal olefins. In the case of ethylene polymerization, polymers prepared from **2**/MMAO or **5**/MMAO are high-density polyethylene, as judged by their T_m values (130.2 and 131.0 °C, respectively), though these are not soluble in refluxing 1,2,4-trichlorobenzene (entry 1 and 4). However, we could not obtain any polyethylene or polypropylene with **4**/$B(C_6F_5)_3$. Nevertheless, **4**/$B(C_6F_5)_3$ shows

Table 4. Polymerization of α-Olefins[a]

entry	cat. (amt, μmol)	monomer	T (°C)	M_n[b]	M_w[b]	M_w/M_n	activity[c]
1[d]	**2** (5.22)	ethylene	28	insol			12.4
2	**2** (5.22)	propylene	28	3110	27400	8.80	3.22
3	**2** (5.22)	1-hexene	28	2120	6990	3.29	0.92
4[e]	**5** (5.02)	ethylene	28	insol			0.71
5	**5** (5.02)	propylene	28	1730	41900	24.2	0.84
6	**5** (5.02)	1-hexene	28	718	5840	8.12	0.31
7	**4** (5.06)	1-hexene	0	11100	56600	5.10	9.25

[a] Conditions: cocatalyst 1000 equiv of MMAO for **2** and **5** and 1 equiv of $B(C_6F_5)_3$ for **4**; 5 min of polymerization. [b] By GPC in 1,2,4-trichlorobenzene vs polystyrene standards; insol = insoluble. [c] 10^4 g of polymer/(mol of catalyst·h). [d] $T_m = 130.2$ °C. [e] $T_m = 131.0$ °C.

a moderate activity in 1-hexene polymerization, which is even better than those of **2**/MMAO or **5**/MMAO. We therefore suspect that deactivation of the active catalytic species in **4**/$B(C_6F_5)_3$ occurs rapidly without substrates or in the presence of ethylene or propylene but the deactivation is relatively slow in the presence of 1-hexene for unknown reasons.

Olefinic resonances are observed in the $^1H/^{13}C$ NMR spectra of the polymers or oligomers prepared with these catalytic systems. For example, the poly(1-hexene) produced by **2**/MMAO (entry 3) shows only terminal olefins (one olefin signal per ~28 monomer units). The molecular weight ($M_n = 2350$) of the polymer estimated by the NMR analysis agrees reasonably well with that by GPC measurement ($M_n = 2120$). All the resulting polypropylenes and polyhexenes are atactic. The low catalytic activities of **2**, **4**, and **5** are presumably due to decomposition of the active catalysts generated with MMAO or $B(C_6F_5)_3$. However, how these catalysts are deactivated is not clear at the moment.

To get some idea of the catalyst activation/deactivation in **4**/$B(C_6F_5)_3$, we monitored the reaction of **4** with $B(C_6F_5)_3$ in the absence of monomers by ^1H and ^{19}F NMR spectroscopy. As $B(C_6F_5)_3$ is added to the toluene-d_8 solution of **4**, the solution turns to brownish red immediately and the signal for the benzylic protons of the chelate ring disappears while the signals for the trimethylsilyl groups are shifted to higher field by ~0.2 ppm. Furthermore, the signal for the methylene protons of the terminal benzyls disappears while a new signal for free toluene, which is apparently liberated during the deactivation process, appears. The liberation of toluene was also observed when the same experiment was done in dichloromethane-d_2 solution. Despite considerable efforts, however, attempts to isolate and characterize the decomposition product have been unsuccessful. Therefore, the activation/deactivation process remains to be established.

In summary, we report titanium and zirconium complexes with the new ancillary diamido ligand MABA that are fully characterized by various means including X-ray crystallography. These titanium and zirconium diamido complexes are easily accessible and serve as precursors for polymerization catalysts for terminal olefins. However, the activities of these catalytic systems are not as high as those of the best known noncyclopentadienyl group 4 metal catalysts, presumably owing to rapid deactivation of the active catalytic species.

Experimental Section

All manipulations were carried out under an inert atmosphere by using a glovebox or standard Schlenk techniques. Solvents were degassed by three freeze−pump−thaw cycles. Pentane, dichloromethane, and chloroform were dried over calcium hydride under argon and vacuum-transferred. Hexane, tetrahydrofuran, toluene, ether, and benzene were vacuum-transferred from their sodium benzophenone ketyl solutions. Deuterated solvents for NMR experiments were dried by the same methods as their nondeuterated analogues. Methyl aluminoxane (MAO) modified with isobutyl groups was purchased as a toluene solution (Akzo, type 4). After the solvent was removed, the solid aluminoxane was dried under vacuum at room temperature for 24 h. Ethylene (99.5+%) and propylene (99+%) gases were purchased from Aldrich and purified by the passage of successive columns of molecular sieves and Redox. NMR spectra were obtained with a Bruker 300 or 500 MHz spectrometer. GPC analyses were carried out on a Waters instrument in 1,2,4-trichlorobenzene (TCB) at 140 °C relative to narrow polystyrene standards (Shodex styrene gel columns). Elemental analyses were performed on a Vario EL elemental analyzer.

H_2(MABA) (1). A solution of 2-aminobenzylamine (4.97 g, 40.66 mmol) in THF (200 mL) was cooled to 0 °C, and then *n*-BuLi (2.5 M in hexane, 34 mL, 85 mmol) was added dropwise over 30 min with stirring. The reaction mixture was warmed to room temperature, and stirring was continued for 12 h. The reaction mixture was then cooled to 0 °C again, and Me_3SiCl (10.5 mL, 81.9 mmol) was added dropwise over 30 min. The ice bath was removed, and the reaction mixture was heated at reflux for 12 h and then stirred at room temperature for an additional 12 h. After removal of the volatile material from the reaction mixture the residue was extracted with pentane (3 × 50 mL). Evaporation of the solvent yielded a brownish liquid which was dried in vacuo and used in the synthesis of metal complexes without further purification (9.93 g, 92%). ^1H NMR ($CDCl_3$): δ 0.15 (s, 9H, $-SiMe_3$), 0.31 (s, 9H, $-SiMe_3$), 0.56 (t, 1H, $-CH_2NH-$), 3.86 (d, 2H, $-NHCH_2-$), 5.18 (bs, 1H, $-C_6H_4NH-$), 6.65−7.14 (m, 4H, $-C_6H_4-$). ^{13}C NMR ($CDCl_3$): δ 0.50 ($-SiMe_3$), 1.27 ($-SiMe_3$), 46.33 ($-NCH_2-$, $J_{C-H} = 133.6$ Hz), 116.76, 117.94, 128.93, 129.03, 130.33, 148.22. MS (HR-EI): *m/e* calcd 266.1635, found 266.1641.

(MABA)$TiCl_2$ (2). To a solution of **1** (1.68 g, 6.32 mmol) in toluene (50 mL) was added 8 mL of *n*-BuLi (1.6 M in hexane, 12.8 mmol) by syringe. The reaction mixture was stirred for 4 h, and $TiCl_4(THF)_2$ (2.18 g, 6.33 mmol) was added to the solution. The reaction mixture was heated at reflux for 3 h and then stirred at room temperature for an additional 12 h. Removal of the volatile materials from the reaction mixture left a dark brown solid which was extracted with pentane (3 × 20 mL). Concentration and cooling (−50 °C) of this solution afforded 415 mg of product (19%) as dark red crystals. ^1H NMR ($CDCl_3$): δ 0.18 (s, 9H, $-SiMe_3$), 0.54 (s, 9H, $-SiMe_3$), 5.32 (s, 2H, $-NCH_2-$), 6.65−7.28 (m, 4H, $-C_6H_4-$). ^{13}C NMR ($CDCl_3$): δ 1.35 ($-SiMe_3$), 2.25 ($-SiMe_3$), 52.79 ($-NCH_2-$, $J_{C-H} = 137.6$ Hz), 116.63, 124.58, 128.34, 128.69, 132.37, 153.57. MS (FAB): 383.07 $(M + H)^+$. Anal. Calcd for $C_{13}H_{24}N_2Si_2Cl_2Ti$: C, 40.77; H, 6.26; N, 7.31. Found: C, 40.85; H, 6.52; N, 7.12.

(MABA)$TiMe_2$ (3). To a solution of **2** (79 mg, 0.21 mmol) in Et_2O was added MeMgI (3.0 M in ether, 0.2 mL, 0.60 mmol) by syringe. The reaction mixture was stirred for 12 h at room temperature. Removal of the volatile materials from the reaction mixture produced a dark black solid which was extracted with hexane (3 × 10 mL). Evaporation of the solvent yielded a sticky solid which was difficult to further purify because of its high solubility even in hydrocarbon solvents. ^1H NMR (C_6D_6): δ 0.26 (s, 9H, $-SiMe_3$), 0.61 (s, 9H, $-SiMe_3$), 1.14 (s, 6H, $Ti-Me$), 4.61 (s, 2H, $-NCH_2-$), 6.95 ~ 7.22 (m, 4H, $-C_6H_4-$). ^{13}C NMR (C_6D_6): δ 0.74 ($-SiMe_3$), 2.05 ($-SiMe_3$),

Table 5. Crystallographic Data for (MABA)TiCl$_2$ (2), (MABA)Ti(CH$_2$Ph)$_2$ (4), and (MABA)$_2$Zr (6)

	2	4	6
formula	$C_{13}H_{24}N_2Si_2Cl_2Ti$	$C_{27}H_{58}N_2Si_2Ti$	$C_{26}H_{48}N_4Si_4Zr$
mol wt	383.32	494.32	620.18
space group	$P2_1/c$	$P2_1/c$	$P\bar{1}$
a, Å	12.619(6)	29.990(6)	10.8312(2)
b, Å	22.784(10)	11.404(2)	17.0329(3)
c, Å	14.269(5)	16.728(4)	19.4166(4)
α, deg	90	90	83.4060(10)
β, deg	105.37(3)	98.07(2)	76.9400(10)
γ, deg	90	90	79.3080(10)
V, Å^3	3956(3)	5664(2)	3418.91(11)
Z	8	4	4
d_{calcd}, g cm^{-3}	1.287	1.160	1.185
radiation (*λ*, Å)	Mo Kα (0.710 73)		
F(000)	1600	2112	1272
μ, cm^{-1}	8.17	4.03	4.81
T, K	188(2)	188(2)	293(2)
scan method	*ω*		
abs cor	semiempirical from *ψ* scans		
no. of measd rflns	15 874	22 033	14 529
no. of indep rflns	6237	8764	9625
refinement method	full-matrix least squares on F^2		
goodness of fit on F^2	1.026	1.045	1.021
final *R* indices ($I > 2\sigma(I)$)	R1 = 0.0348, wR2 = 0.0823	R1 = 0.0514, wR2 = 0.1016	R1 = 0.0239, wR2 = 0.0611
R indices (all data)	R1 = 0.0528, wR2 = 0.0922	R1 = 0.0928, wR2 = 0.1228	R1 = 0.0280, wR2 = 0.0630

30.69 (Ti−*Me*), 52.23 (−N*C*H$_2$−), 119.44, 121.32, 125.81, 129.45, 135.97, 151.85.

(MABA)Ti(CH$_2$Ph)$_2$ (4). To a solution of **2** (90 mg, 0.24 mmol) in diethyl ether (30 mL) was added dropwise 0.5 mL of PhCH$_2$MgCl (1.0 M in diethyl ether, 0.5 mmol). The reaction mixture was stirred for 12 h at room temperature. After removal of the volatile materials, the reaction mixture was extracted with pentane. The extract was concentrated to nearly 1 mL and cooled to −50 °C to produce a reddish purple crystalline solid which was collected and dried under vacuum (105 mg, 90%). ^{1}H NMR (CDCl$_3$): *δ* 0.07 (s, 9H, −Si*Me*$_3$), 0.27 (s, 9H, −Si*Me*$_3$), 2.43 (d, 2H, J_{H-H} = 10.5 Hz, Ti−CH*H*Ph), 2.59 (d, 2H, J_{H-H} = 10.5 Hz, Ti−C*H*HPh), 4.58 (s, 2H, N−C*H*$_2$), 6.84−7.15 (m, 14H, −CH$_2$C$_6$*H*$_5$, −C$_6$*H*$_4$−). ^{13}C NMR (CDCl$_3$): *δ* 1.44 (−Si*Me*$_3$), 2.79 (−Si*Me*$_3$), 52.19 (−N*C*H$_2$−, J_{C-H} = 135.7 Hz), 82.55 (Ti−*C*H$_2$Ph, J_{C-H} = 123.4 Hz), 120.74, 122.20, 123.38, 127.67, 128.18, 128.71, 129.47, 137.10, 147.31, 152.50. Anal. Calcd for $C_{27}H_{38}N_2Si_2Ti$: C, 65.59; H, 7.69; N, 5.67. Found: C, 64.67; H, 7.57; N, 5.67. Despite several trials with crystalline materials, a low carbon content was found in the elemental analysis.

(MABA)$_2$Zr (6). To a solution of **1** (1.38 g, 5.16 mmol) in hexane (30 mL) was added 6.8 mL of *n*-BuLi (1.6 M in hexane, 10.9 mmol) by syringe. The reaction mixture was stirred for 12 h, and the volatiles were removed under vacuum. The residue was dissolved in toluene (30 mL), and ZrCl$_4$(THF)$_2$ (2.10 g, 5.57 mmol) was added to the solution. The reaction mixture was heated at reflux for 3 h and then stirred at room temperature for an additional 12 h. Removal of the volatile materials from the reaction mixture left a brownish white solid which was extracted with pentane (3 × 20 mL). Concentration and cooling (−50 °C) of this solution afforded 675 mg of product (42%) as colorless crystals. ^{1}H NMR (CDCl$_3$): *δ* 0.07 (s, 18H, −Si*Me*$_3$), 0.21 (s, 18H, −Si*Me*$_3$), 4.22 (d, 2H, −NCH*H*−, J_{H-H} = 15.3 Hz), 4.53 (d, 2H, −NCH*H*−, J_{H-H} = 15.3 Hz), 6.80−7.14 (m, 8H, −C$_6$*H*$_4$−). ^{13}C NMR (CDCl$_3$): *δ* 1.67 (−Si*Me*$_3$), 2.71 (−Si*Me*$_3$), 50.43 (−N*C*H$_2$−), 121.21, 124.04, 129.03, 129.86, 136.56, 151.04. Anal. Calcd for $C_{26}H_{48}N_4Si_4Zr$: C, 50.38; H, 7.74; N, 9.04. Found: C, 49.41; H, 7.84; N, 8.75. Despite several trials with crystalline materials, a low carbon content was found in the elemental analysis.

(MABA)ZrCl$_2$·THF (5). ZrCl$_4$(THF)$_2$ (403 mg, 1.07 mmol) was added to a toluene solution of **6** (545 mg, 0.88 mmol). The reaction mixture was refluxed for 3 days. Removal of volatile components gave a yellowish residue which was extracted with diethyl ether. Concentration and cooling (−50 °C) of this solution afforded 200 mg of product (46%) as yellowish crystalline materials. ^{1}H NMR (CDCl$_3$): *δ* 0.04 (s, 9H, −Si*Me*$_3$), 0.43 (s, 9H, −Si*Me*$_3$), 1.97 (t, *THF*, 4H), 4.14 (t, *THF*, 4H), 4.82 (s, 2H, −NC*H*$_2$−), 6.79−7.15 (m, 4H, −C$_6$*H*$_4$−). ^{13}C NMR (CDCl$_3$): *δ* 0.79 (−Si*Me*$_3$), 1.62 (−Si*Me*$_3$), 25.84 (*THF*), 48.53 (−N*C*H$_2$−), 72.91 (*THF*), 120.61, 120.91, 128.24, 128.31, 133.49, 151.50. Anal. Calcd for $C_{13}H_{24}N_2Si_2Cl_2Zr{\cdot}C_4H_8O$: C, 40.96; H, 6.42; N, 5.62. Found: C, 40.58; H, 6.49; N, 5.17.

Polymerization with 2 and MMAO. A stock solution (10.44 mM in toluene) of **2** (0.5 mL, 5.22 *μ*mol) and MMAO (310 mg, 5.35 mmol) were added to toluene to make the volume of the solution 20 mL. After the solution was stirred for 20 min, ethylene or propylene gas was bubbled into the solution for 5 or 30 min with vigorous stirring at room temperature. The polymerization was quenched with acidic methanol. In the case of 1-hexene polymerization, 2 mL of monomer was added to 18 mL of the toluene solution containing the same amounts of **2** and MMAO as above. After 5 min of stirring, the reaction was quenched with acidic methanol. The resulting polymer and/or oligomer was isolated by the general workup procedure and dried under vacuum, which gave 54 mg of PE, 14 mg of PP, and 4 mg of PH within 5 min. The polymerization with a longer period of time (30 min) did not improve the yield. Molecular weights of the samples were estimated by GPC measurement.

Polymerization with 5 and MMAO. The same procedure as above was employed, except that a stock solution (10.03 mM in toluene) of **5** (0.5 mL, 5.02 *μ*mol) and MMAO (290 mg, 5.00 mmol) were used and polymerization was carried out for 5 min at ambient temperature.

Polymerization with 4 and B(C$_6$F$_5$)$_3$. The same procedure as above was employed, except that a stock solution of **4** (10.12 mM in toluene; 0.5 mL, 5.06 *μ*mol) and B(C$_6$F$_5$)$_3$ (10.16 mM in toluene; 0.5 mL, 5.08 *μ*mol) were used and polymerization was carried out for 5 min at 0 °C. In the case of ethylene or propylene polymerization, 10 equiv of triisobutylaluminum (TIBA) was added as scavenger, but no polymerization products were obtained. In the case of 1-hexene polymerization, 39 mg of atactic poly(1-hexene) was obtained within 5 min.

NMR Experiment on 4/B(C$_6$F$_5$)$_3$. Complex **4** (20 mg, 40.5 *μ*mol) was dissolved in 0.5 mL of toluene-*d*$_8$, and the ^{1}H spectrum was recorded. ^{1}H NMR (toluene-*d*$_8$, 25 °C): *δ* 0.26 (s, 9H, −Si*Me*$_3$), 0.46 (s, 9H, −Si*Me*$_3$), 2.76 (d, 2H, −*C*H$_2$Ph), 2.92 (d, 2H, −*C*H$_2$Ph), 4.73 (s, 2H, −N*C*H$_2$−), 6.95−7.35 (m, 14H, −Ph). ^{1}H and ^{19}F NMR spectra were obtained after the addition of 1.0 equiv of B(C$_6$F$_5$)$_3$ to **4**. The initial yellowish red solution immediately turned to brownish red. The ^{1}H NMR spectrum taken after a few minutes of the borane addition shows the higher field shift of trimethylsilyl groups by ~0.2 ppm: δ 0.05 (s, 9H, $-$SiMe_3), 0.27 (s, 9H, $-$SiMe_3). The increased toluene signal at 2.30 ppm indicates the liberation of free toluene. Other parts of the ^{1}H NMR spectrum are too complex to assign unambiguously. However, the ^{19}F NMR spectrum shows one fluorinated benzene ring: ^{19}F NMR (toluene-d_8) δ -56.31 (d, 2F), -86.88 (m, 1F), -90.94 (m, 2F). Despite considerable efforts, attempts to isolate and characterize the decomposition product have been unsuccessful.

X-ray Crystallography. A suitable crystal coated with Paratone was mounted on a Siemens SMART diffractometer equipped with a graphite-monochromated Mo Kα ($\lambda = 0.710\,73$ Å) radiation source and a CCD detector. Data collection was performed with a detector distance of 6 cm. For each structure, a total of 1271 frames of two-dimensional diffraction images were collected. The raw data collected were processed to produce conventional intensity data by the program SAINT. The intensity data were corrected for Lorenz and polarization effects. Absorption correction was also applied on the basis of ψ scans. The structure was solved by a combination of Patterson and difference Fourier methods provided by the program package SHELEXTL. All the non-hydrogen atoms were refined anisotropically. Hydrogen atom positions were calculated and included in the final cycle of refinement. However, for **2**, which shows an agostic interaction between C(7)$-$H or C(20)$-$H and the Ti center, the hydrogens attached to C(7) and C(20) were located from the difference electron density map and refined isotropically. Crystallographic data of the compounds **2**, **4**, and **6** are summarized in Table 5.

Acknowledgment. We gratefully acknowledge the Korea Science and Engineering Foundation for support of this work. We also thank Dr. Jaheon Kim for help in X-ray work and Professor G. V. Smith for reading the manuscript.

Supporting Information Available: Structural diagrams with full atom labeling and tables of bond distances, angles, anisotropic thermal parameters, and atomic coordinates for **2**, **4**, and **6**. This material is available free of charge via the Internet at http://pubs.acs.org.

OM990121B